FREQUENCY- AND WAVE-VECTOR-DEPENDENT LONGITUDINAL MICROSCOPIC DIELECTRIC FUNCTION AND ENERGY LOSS SPECTRUM FOR COPPER. II

Abu El-Hassan S. Seoud

Physics Department
Faculty of Science, Tanta University
Tanta, Egypt

الخلاصة :

تـمّ في هذه الدراسة حساب دالة العزل الميكروسكوبية الطولية المعتمدة على التردد والمتجه الموجي للنحاس لمتجهات موجيّة في الاتجاهين البلوريْـن الاساسيـن [٠٠١] و [١١١] لطاقات بين (٢ و ٤) رودبرج . ولقد استخدمنا طريقة الموجات المستوية الزائدة المُـعَـدَّلة (MAPW) مع جهد شودوروف لحساب الدوال الموجيّة والقيم الذاتية للطاقة .

ولقد وجدنا ذروة في طيف فَـقْد الطاقة (ELS) عند (٢,١) رودبرج والتي تتحرك في اتجاه الطاقة الاعلى مع زيادة القيمة العددية للمتجه الموجى ، كذلك أجرينا مقارنة بين نتائجنا في هذه الدراسة ونتائجنا السابقة .

ABSTRACT

The longitudinal microscopic frequency- and wave-vector-dependent dielectric function $\varepsilon(q, \omega)$ is calculated for copper for wave vectors in the two main crystallographic directions namely, [100] and [111] for energies $2 < \hbar\omega \leq 4$ Rydberg. The energy eigenvalues and wave functions which are used have been obtained from realistic energy-band calculations based on the modified augmented plane wave (MAPW) method with Chodorow potential.

A peak is found in the energy loss spectrum (ELS) at 2.1 Rydberg which moves gradually to high energy side with increasing $|q|$. A comparison is made between the present results and our previous calculations.

FREQUENCY- AND WAVE-VECTOR-DEPENDENT LONGITUDINAL MICROSCOPIC DIELECTRIC FUNCTION AND ENERGY LOSS SPECTRUM FOR COPPER(II)

1. INTRODUCTION

Earlier papers in this series [1–4] have been concerned with the interpretation of the complex dielectric function (CDF) and energy loss spectrum (ELS) of copper in the main crystallographic directions, namely, [100], [110], and [111] in two ranges of energies, $2 < \hbar\omega \leq 4$ Rydberg, [1, 2] (1 Ry = 13.6058 eV) and $8 < \hbar\omega \leq 10$ Ry [2, 3, 4]; also, we have studied [5] the behavior of both CDF and ELS in the three above-mentioned crystallographic directions in the range of energies $0 < \hbar\omega \leq 2$ Ry.

We want in this paper to survey the CDF and ELS of copper through some choosed calculations at the range of energies $2 < \hbar\omega \leq 4$ Ry in two crystallographic directions, namely, [100] and [111].

2. METHOD OF CALCULATIONS

We have given in our previous work [4] (hereafter referred to as Part I) the main equations about the MAPW-wave functions, the matrix elements such as $\langle b', \mathbf{k}+\mathbf{q}+\mathbf{G}^* | \exp(i\mathbf{q}\cdot\mathbf{r}) | b, \mathbf{k} \rangle$ and the longitudinal microscopic dielectric function. For the purpose of numerical calculations and integration in $\mathbf{k}$-space the longitudinal microscopic dielectric function can be written as [5]:

$$E_{b, \mathbf{k}_i+\mathbf{s}} = E_{b\mathbf{k}_i} + \mathbf{s} \text{ grad } E_{b\mathbf{k}_i}; \quad \mathbf{k} = \mathbf{k}_i + \mathbf{s} . \quad (2)$$

The weight factors $g(\mathbf{k}_i)$ satisfy the relation,

$$\sum_{\mathbf{k}_i \in \text{IRBZ}} g(\mathbf{k}_i) = 1 \quad (3)$$

In practice, each cube must be weighted appropriately to give the correct effective volume of integration W_i [7]. Thus the problem is reduced to the evaluation of the following integrals:

$$I_1 = \int_W \frac{\Theta(A + B_1 x + B_2 y + B_3 z)}{C + u_1 x + u_2 y + u_3 z} \, dx \, dy \, dz \quad (4)$$

$$I_2 = \int_W \Theta(A + B_1 x + B_2 y + B_3 z)$$
$$\times \, \delta(C + u_1 x + u_2 y + u_3 z) \, dx \, dy \, dz , \quad (5)$$

with

$$A = E_F - E_{b\mathbf{k}}$$
$$\mathbf{B} = -\nabla E_{b\mathbf{k}}$$
$$C = E_{b\mathbf{k}} - E_{b', \mathbf{k}+\mathbf{q}} \pm \hbar\omega$$
$$\mathbf{u} = \nabla(E_{b\mathbf{k}} - E_{b', \mathbf{k}+\mathbf{q}}) . \quad (6)$$

For the fine details of evaluation of both $\mathbf{k}$-space integrals and the used subroutines see references [5–7].

$$\varepsilon(\mathbf{q}+\mathbf{G}, \mathbf{q}+\mathbf{G}', \omega) = \delta_{\mathbf{G}, \mathbf{G}'} - \frac{4e^2}{\pi^2} - \left(\frac{2\pi}{a}\right)^3 \frac{1}{|\mathbf{q}+\mathbf{G}|^2}$$

$$\times \sum_{\mathbf{k}_i \in \text{IRBZ}} \sum_{b, b'} \sum_{\beta} g(\mathbf{k}_i) \, \langle b\mathbf{k}_i | \exp\{-i\beta^{-1}(\mathbf{q}+\mathbf{G})\cdot\mathbf{r}\} |$$

$$\times \, b', \mathbf{k}_i + \beta^{-1}(\mathbf{q}+\mathbf{G}^*) \rangle \langle b', \mathbf{k}_i + \beta^{-1}(\mathbf{q}+\mathbf{G}^*) | \exp\{-i\beta^{-1}(\mathbf{q}+\mathbf{G}')\mathbf{r}\} | b\mathbf{k}_i \rangle$$

$$\times V_{\text{cube}}^{-1} \left\{ \int_{W_i} d^3s \, \frac{\Theta(E_F - E_{b\mathbf{k}_i} - \mathbf{s}\cdot\nabla E_{b\mathbf{k}_i}}{E_{b\mathbf{k}_i} - E_{b', \mathbf{k}_i+\beta^{-1}\mathbf{q}} + \hbar\omega + \mathbf{s}\cdot\nabla(E_{b\mathbf{k}_i} - E_{b', \mathbf{k}_i+\beta^{-1}\mathbf{q}}) + i\eta} \right.$$

$$\left. + \int_{W_i} d^3s \, \frac{\Theta(E_F - E_{b\mathbf{k}_i} - \mathbf{s}\cdot\nabla E_{b\mathbf{k}_i}}{E_{b\mathbf{k}_i} - E_{b', \mathbf{k}_i+\beta^{-1}\mathbf{q}} - \hbar\omega + \mathbf{s}\cdot\nabla(E_{b\mathbf{k}_i} - E_{b', \mathbf{k}_i+\beta^{-1}\mathbf{q}}) - i\eta} \right\} , \quad (1)$$

with the same definitions as given in Part I. β is that element of the cubic point group which projects the vector $\mathbf{k}+\mathbf{q}+\mathbf{G}^*$ into the irreducible wedge, IRBZ, $k_x \geq k_y \geq k_z \geq 0$. E_F is the Fermi level. By using the weighting factors $g(\mathbf{k}_i)$ the dielectric function may be expressed by sums of integrals, each of them extended over one cube of volume V_{cube} [6]. Inside each cube the matrix elements are approximated by their values at the center of the cube, $\mathbf{k}_i$, whereas the energies are approximated by a Taylor expansion up to the linear terms [7].

3. RESULTS AND DISCUSSION

We have choosen for the present work three P-vectors in the two main crystallographic directions, namely, [100] and [111] for energies $2 < \hbar\omega \leq 4$ Ry. Table 1 gives the corresponding values for q and G for these P-vectors in units of $2\pi/a$.

We have found [5] for these P-vectors the peaks in the ELS, whose energy position is given in Table 2.

It is well known today [5, 8] that the characteristic energy loss spectrum of copper is not free-electron-like,

Table 1. P = q + G in Units of 2π/a

P	q	G
(¼, 0, 0)	(¼, 0, 0)	(0, 0, 0)
(½, ½, ½)	(½, ½, ½)	(0, 0, 0)
(3, 0, 0)	(1, 0, 0)	(2, 0, 0)

Table 2. The Energy Position (Ry) in the ELS for Energies $0 < \hbar\omega \leq 2$ Ry as Calculated in Reference [5].

P	First Peak	Second Peak
(¼, 0, 0)	1.39	1.87
(½, ½, ½)	1.65	1.85
(3, 0, 0)	1.68	—

but its character is ascribed to the interband transition from the 3d-bands to the empty bands.

Figure 1 shows the ELS of copper for energies $2 < \hbar\omega \leq 4$ Ry for the mentioned above P-vectors. The fixed peak at about 2.1 Ry for both $q = (¼, 0, 0)$ $(2\pi/a)$ and $q = (½, ½, ½)$ $(2\pi/a)$ was found also in the [110]-direction [1], which proves that this peak is fixed one in the characteristic energy loss spectrum of copper. The position of this peak is moved to about 2.3 Ry for $P = (3, 0, 0)$ $(2\pi/a)$. The gradual movement of the peaks to high energy side with increasing $|q|$ was also noticed [1, 5, 8].

We believe that the 2.8-peak in the ELS which appears in the case of $P = (3, 0, 0)$ $(2\pi/a)$ is a numerical error which appears also in the calculations of both real and imaginary parts (see Figures 6 and 7). The expected origin of such an error is discussed later.

One can also notice that the real part has nothing to do with the shape of the ELS for $P = (3, 0, 0)$ $(2\pi/a)$ ($\varepsilon_1 \approx 1$ and ε_2 is small; then $Im(-\varepsilon^{-1}) \approx \varepsilon_2$). This can also be seen by comparing Figures 1c and 7. This straightforward behavior of the ELS is due to the excitation of core electrons [9].

Figures 2–7 show the real part, ε_1, dotted curves, and the imaginary part, ε_2, dot-broken curves, with the same notations as in Part I.

3.1. Comparison with Experiments

Since the theoretical calculations of neither $\varepsilon(q, \omega)$ nor the energy loss spectrum results exist presently
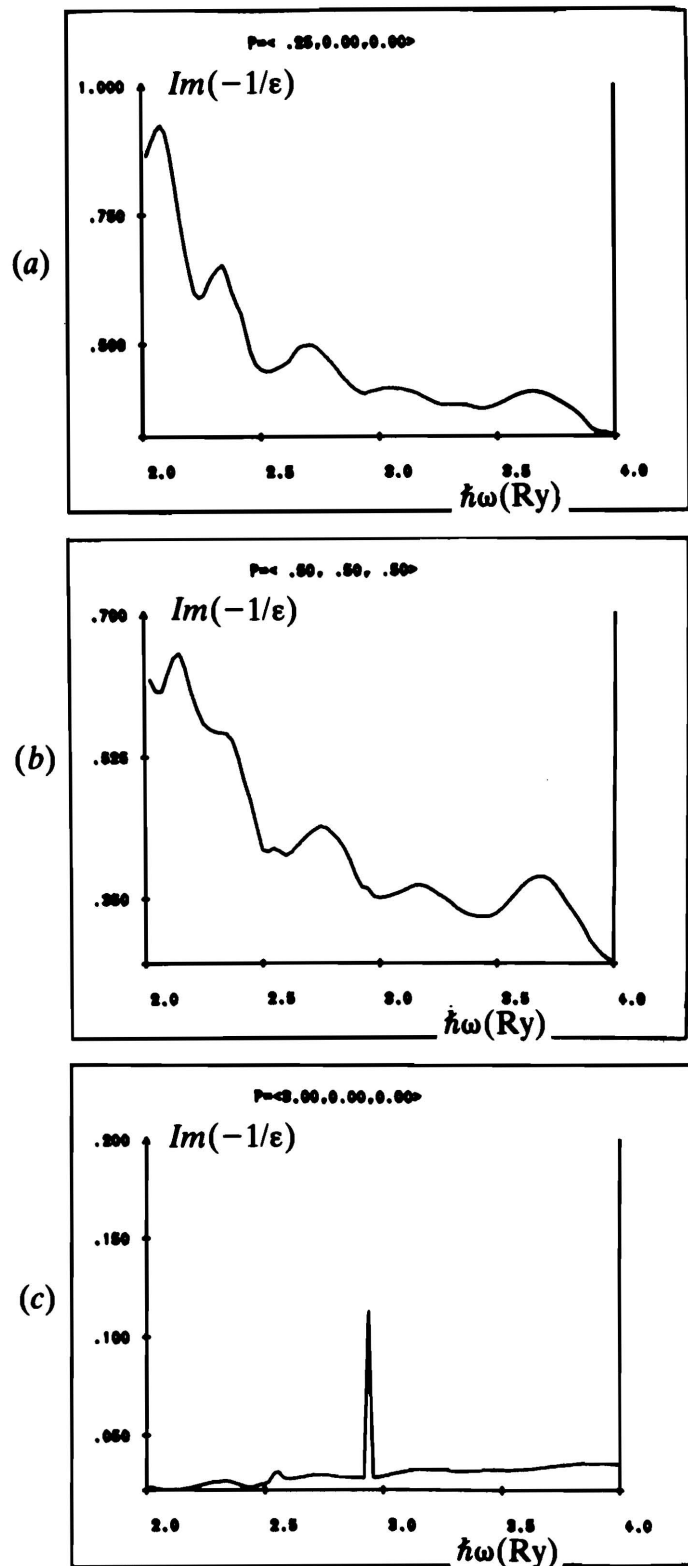

Figure 1. The Imaginary Part of the Inverse Dielectric Function, $Im(-1/\varepsilon)$.
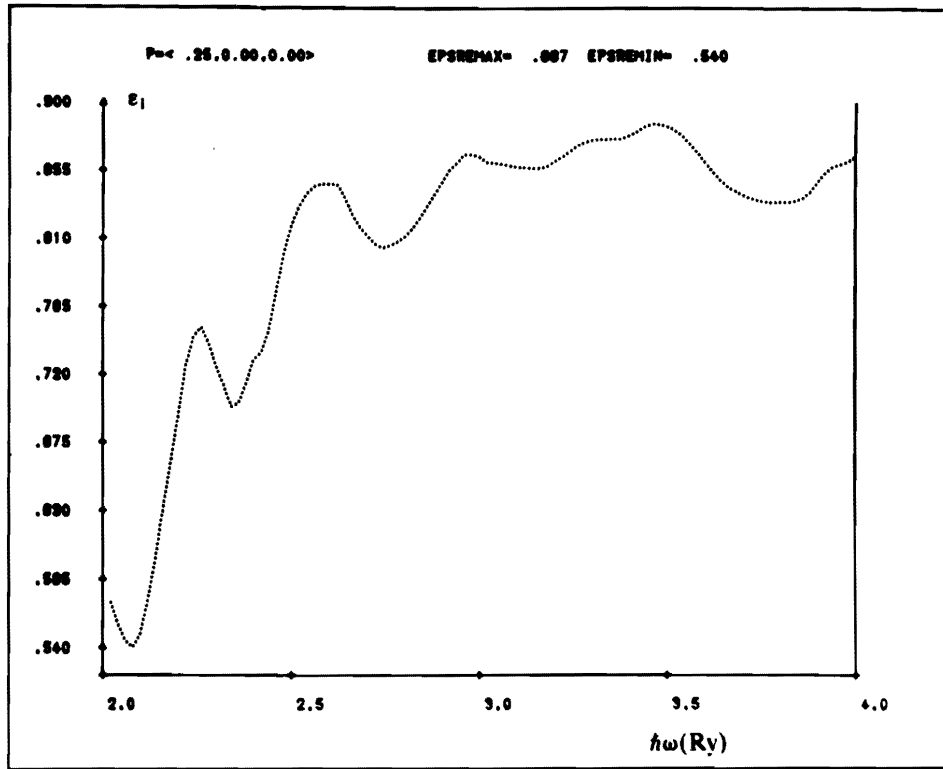*(a)* $q = (¼, 0, 0)$ $(2\pi/a)$; *(b)* $q = (½, ½, ½)$ $(2\pi/a)$; *(c)* $P = (3, 0, 0)$ $(2\pi/a)$.

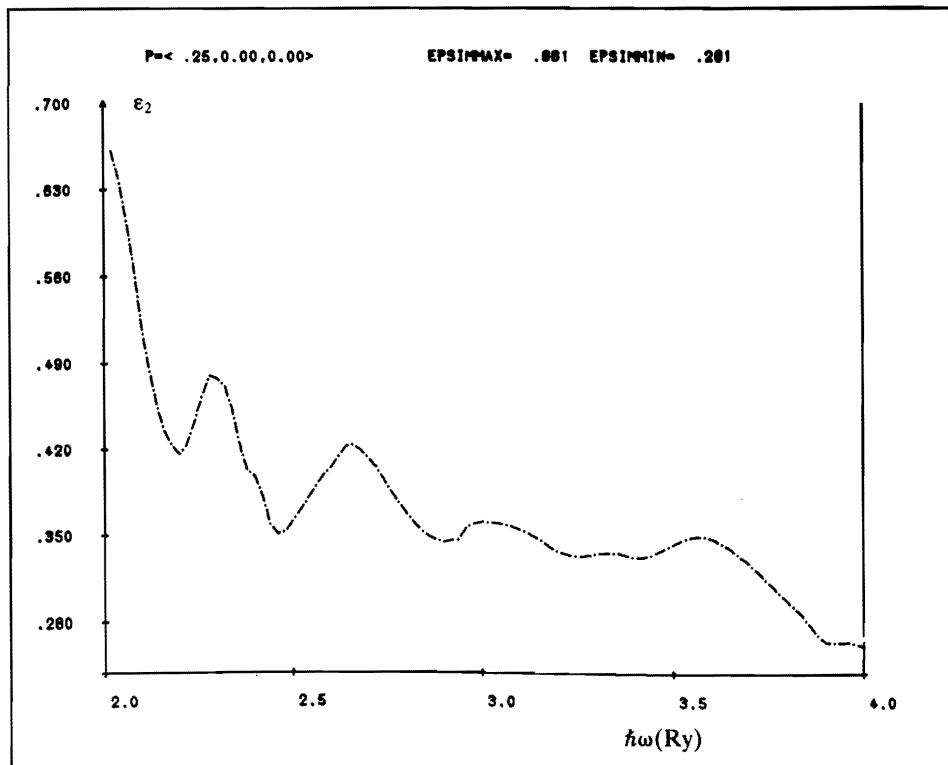*Figure 2. The Real Part $\varepsilon_1(q, \omega)$ for $q = (1/4, 0, 0) (2\pi/a)$.*

Figure 3. The Imaginary Part $\varepsilon_2(q, \omega)$ for $q = (1/4, 0, 0) (2\pi/a)$.

Figure 4. The Real Part $\varepsilon_1(\mathbf{q}, \omega)$ for $\mathbf{q} = (\frac{1}{2}, \frac{1}{2}, \frac{1}{2}) (2\pi/a)$.
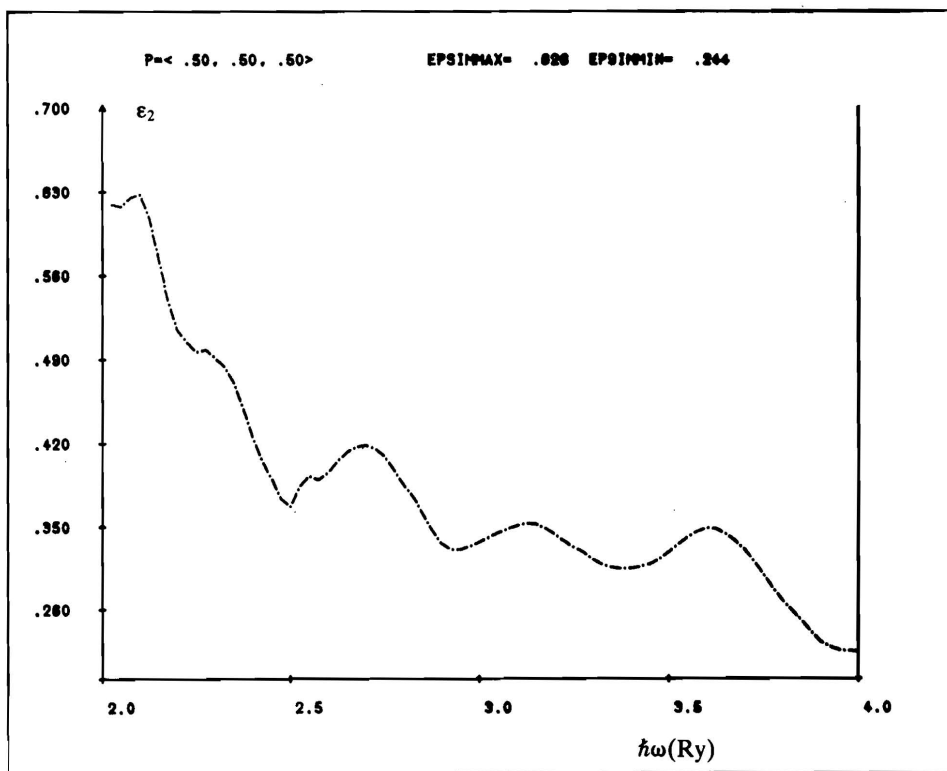
Figure 5. The Imaginary Part $\varepsilon_2(\mathbf{q}, \omega)$ for $\mathbf{q}= (\frac{1}{2}, \frac{1}{2}, \frac{1}{2}) (2\pi/a)$.
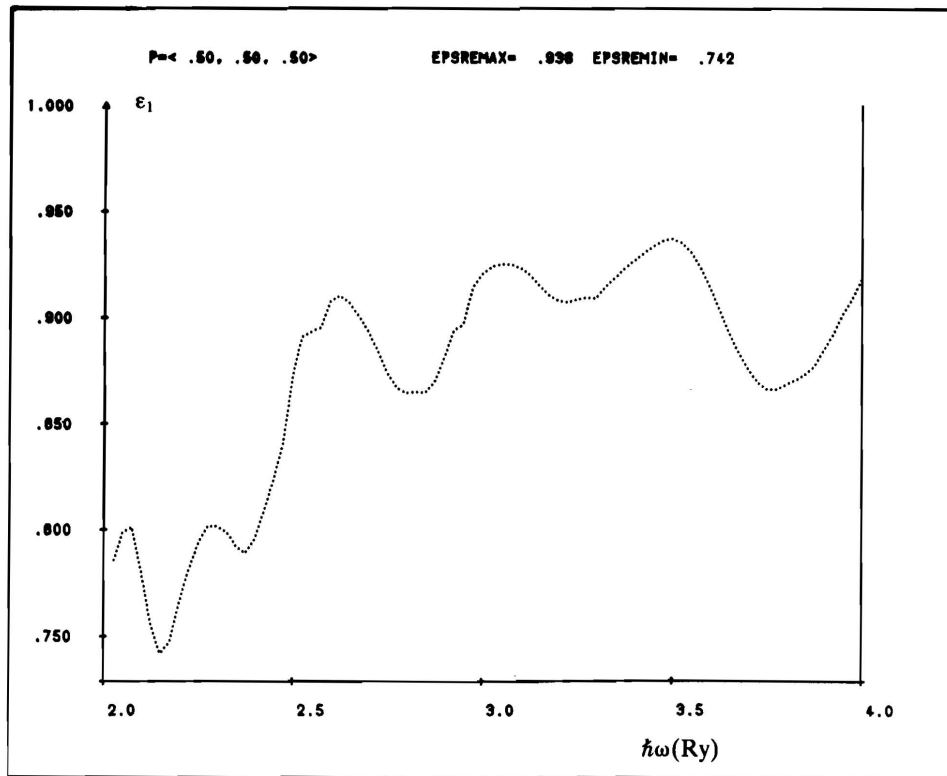
Figure 6. The Real Part $\varepsilon_1(\mathbf{q}, \omega)$ for $\mathbf{P} = (3, 0, 0)$ $(2\pi/a)$.

Figure 7. The Imaginary Part $\varepsilon_2(\mathbf{q}, \omega)$ for $\mathbf{P} = (3, 0, 0)$ $(2\pi/a)$.
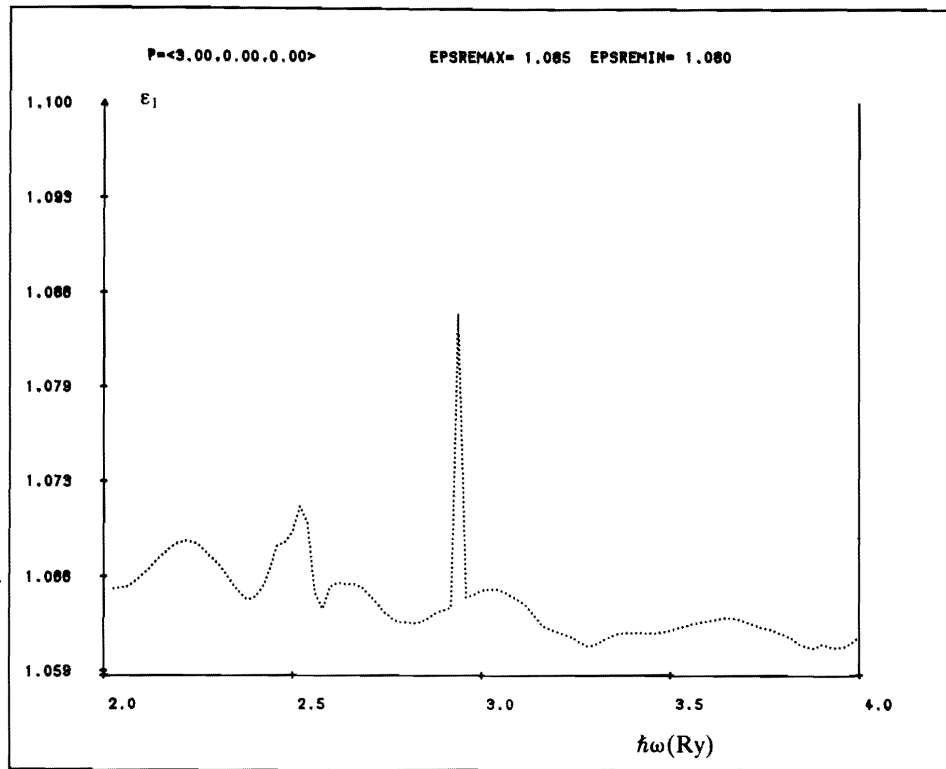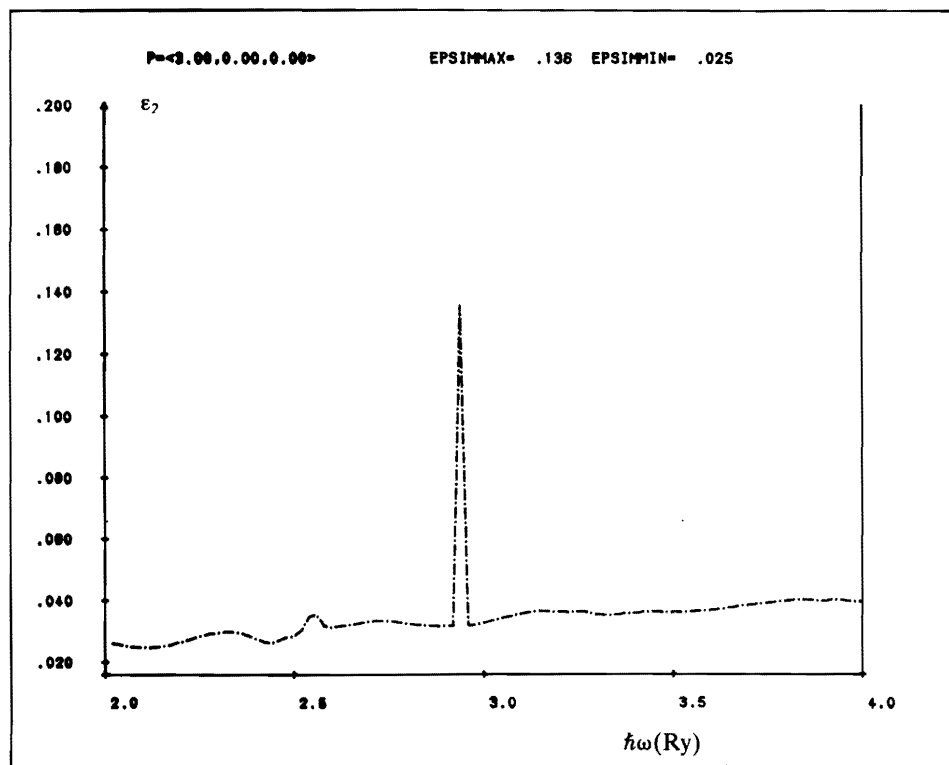
for this energy range, our comparison with experiment can only be qualitative. Let us make the trick, to be able to use the experimental available data. If we take our results for $q = (\frac{1}{4}, 0, 0)$ $(2\pi/a)$ and forget for instance the q-dependence of ε, *i.e.* $\varepsilon(q, \omega) \approx \varepsilon(\omega)$ [9]. This is reasonable in our case because $|q|$ is small compared with the smallest reciprocal lattice vector in this direction, $G_o = (2, 0, 0)$ $(2\pi/a)$. The expected relative error in the ELS owing to this assumption is less than 8% [5], which lie within the experimental error. Also the energy loss spectroscopy experiments are mainly done in the optical region, *i.e.*, $|q| \approx 0$. Now we can avoid the lacking of q-dependent calculations or experimental results in this energy region. For example we will calculate the absorption coefficient, μ, at certain energies and compare our results with other workers; μ is given as [10]:

$$\mu = \frac{2\omega}{c} \{ \frac{1}{2} [(\varepsilon_1^2 + \varepsilon_2^2)^{1/2} - \varepsilon_1] \}^{1/2} . \tag{7}$$

In Table 3, we give our calculated results according to Equation (7) from our results for ε_1, Figure 2, and ε_2, Figure 3, as present work compared with other results, in units of 10^5 cm^{-1}.

Table 3. Comparison of the Absorption Coefficient (μ) with Other Work in Units of 10^5 cm^{-1}.

$\hbar\omega$ (Ry)	Present Work	HKS [11]	SHK [12]	WG [13]
2.06	10.6	—	—	9.0
3.10	8.3	7.7	7.7	5.8
4.00	6.4	6.7	6.7	5.2

From Table 3, one can see that our values of μ are in reasonable agreement with the tabulated values, taken into account that those of HKS (or SHK) are 20–40% higher than from WG [13].

From Figure 1, we can see that there are five common peaks in our ELS which are tabulated in Table 4.

The 2.06 Ry peak is very famous in the literature (see for example reference [14] and references therein) this peak moves gradually as $|q|$ becomes greater which is noticed also in the [110] direction [1]. The other peaks in ELS move also to high energy side but some of them are decayed (see Table 4). The movement of peaks in the ELS to high energy side is noticed also from Kubo [8] and Seoud [5]. The stability of some peaks and the movement of others can be explained in the basis of the band structure of copper as a result of electron transitions between broad maxima and minima as for example near the L-point.

As noted by Wehenkel [15] peaks in the density of oscillator strength $f(E)$ in this energy range occur near minima of ELS. Due to Feldkamp and others [14], their $f(E)$ curve has two minima at 3.09 and 3.67 Ry. Those values are in very good agreement with the fourth and fifth ELS-peaks for $q = (\frac{1}{4}, 0, 0)$ $(2\pi/a)$, (see Figure 1a). Moreover Wehenkel and Gauthé [10] proved that peaks in μ are due to slope change in ε_2-curve and to a shoulder in ε_1-curve which appears in the same energy range. According to the μ-curves of HKS [11], HGK [16] and WG [13], there is a peak at 3.09 Ry which is very clear in the HKS-curve and much weaker in the WG-curve. Another μ-peak is situated at 3.45 Ry in the HGK [16]-curve, which is not clear in the other two curves. On examining ε_1 and ε_2 curves, Figures 2 and 3, it can be observed that both features are very clear near 3.1 Ry and 3.45 Ry, which indicates that there are μ-peaks around those energies.

3.2 Sources of Errors in k-Space Integration

The sources of error in the k-space integration are well known, but it is very difficult to make any quantitative estimate of these errors [17].

Table 4. ELS Peaks for $2 < \hbar\omega \leqslant 4$ Ry.

P/$(2\pi/a)$	Energy Position (Ry)				
	First Peak	Second Peak	Third Peak	Fourth Peak	Fifth Peak
$(\frac{1}{4}, 0, 0)$	2.06	2.33	2.70	3.09	3.64
$(\frac{1}{2}, \frac{1}{2}, \frac{1}{2})$	2.13	Decayed	2.73	3.14	3.68
$(3, 0, 0)$	2.31	2.52	Decayed	Decayed	Decayed

One of the most important sources of error in the k-space integrations is that associated with the possible degeneracies in the energy eigenvalues which caused troubles in the calculations of energy gradients (but see reference [18] which avoid such problems in the calculations). The second error is associated with the linear approximation of the band structure inside the cubes (Equation 2).

For other sources of numerical errors and how can one overcome this problem, see references [5, 17].

3.3. The Time Needed for Our Calculations

Table 5 gives the computational time needed for the calculation of the dielectric function ε per energy $\hbar\omega$ at computer model "CYBER 175" for the three main crystallographic directions [100], [110], and [111], and also the computational time for the matrix elements $\langle \exp i(q+G)\cdot r \rangle$.

Table 5. The Computational Time in Seconds.

Direction	The Matrix Elements $\langle \exp i(q+G)\cdot r \rangle$ (75×75)	Time for ε per $\hbar\omega$
[100]	30	50
[110]	30	100
[111]	30	65

ACKNOWLEDGEMENT

REFERENCES

[1] A. Seoud, "The Behaviour of the Complex Dielectric Function and Energy Loss Spectrum of Copper at [110]-Direction at the Range of Energies $2 < \hbar\omega \leq 4$ Rydberg", *Journal of Materials Science*, **23** (1988), in press.

[2] A. Seoud and F. Khater, "New Peaks at Copper Energy Loss Spectrum in the [111]-Direction", *Philosophical Magazine*, in press.

[3] A. Seoud, "The Energy Loss Spectrum of Copper for Energies $8 < \hbar\omega \leq 10$ Rydberg in the [100]-Direction", to be published.

[4] A. Seoud, "Frequency- and Wave-Vector-Dependent Longitudinal Microscopic Dielectric Function and Energy Loss Spectrum for Copper. I", *Arabian Journal for Science and Engineering*, **13**(1) (1988), p. 87.

[5] A. Seoud, "Berechnung der Longitudinalen Mikroscopischen Dielektrischen Funktion und Energieverlustfunktion von Kupfer", *Doctoral Thesis, Ludwig-Maximilians University, Munich,* 1983.

[6] H. Bross, "Pseudopotential Theory of the Dielectric Function of Al—the Volume Plasmon Dispersion", *Journal of Physics F: Metal Physics,* **8** (1978), p. 2631.

[7] J. Diamond, "Computational Method for Generalized Susceptibility", (1971) in *Computational Methods in Band Theory,* The IBM Research Symposia Series, New York.

[8] Y. Kubo, S. Wakoh, and J. Yamashita, "Energy Loss Spectrum of Copper", *Journal of the Physical Society of Japan,* **41** (1976), p. 1556.

[9] C. Kittel, *Introduction to Solid State Physics.* 5th edn., New Delhi: Wiley Eastern, 1984, p. 323.

[10] C. Wehenkel and B. Gauthé, "Electron Energy Loss Spectra and Optical Constants of Bismuth", *Solid State Communications,* **15** (1974), p. 555.

[11] R. Haensel, C. Kunz, and B. Sonntag, *Physics Letters,* **25A** (1967), p. 205.

[12] B. Sonntag, R. Haensel, and C. Kunz, *DESY 69/6,* January 1969.

[13] C. Wehenkel and B. Gauthé, "Optical Absorption Coefficient of Nickel, Palladium, Platinum and Copper, Silver, Gold Between 20 and 120 eV", *Optics Communications,* **11** (1974), p. 62.

[14] L. Feldkamp, L. Davis, and M. Stearns, "Analysis of Electron Inelastic—Scattering Data with Application to Cu", *Physical Review B,* **15** (1977), p. 5535.

[15] C. Wehenkel, *Journal de Physique,* **36** (1975), p. 199.

[16] H. Hagemann, W. Gudat, and C. Kunz, "Optical Constants from the Far infrared to the X-ray Region: Mg, Al, Cu, Ag, Au, Bi, C and Al_2O_3", *Journal of the Optical Society of America,* **65** (1975), p. 742.

[17] G. Gilat and L. Raubenheimer, "Accurate Numerical Method for Calculating Frequency-Distribution Functions in Solids", *Physical Review,* **144** (1966), p. 390.

[18] J. Rath and A. Freeman, "Generalized Magnetic Susceptibilities in Metals: Application of the Analytic Tetrahedron Linear Energy Method to SC", *Physical Review B,* **11** (1975), p. 2109.